



# Evaluation of sesamol-induced histopathological, biochemical, haematological and genomic alteration after acute oral toxicity in female C57BL/6 mice



Shahanshah Khan<sup>a,b</sup>, Sandeep Choudhary<sup>a</sup>, Arun Kumar<sup>a</sup>, Akanchha Mani Tripathi<sup>a</sup>, Amit Alok<sup>a</sup>, Jawahar Singh Adhikari<sup>a</sup>, Moshahid Alam Rizvi<sup>b,\*</sup>, Nabo Kumar Chaudhury<sup>a,\*</sup>

<sup>a</sup> Division of Radiation Biodosimetry, Institute of Nuclear Medicine and Allied Sciences, Defence Research & Development Organization, Brig. S. K. Mazumdar Marg, Timarpur, Delhi 110054, India

<sup>b</sup> Department of Biosciences, Faculty of Natural Sciences, Jamia Millia Islamia—A Central University, Moulana Mohammad Ali Jauhar Marg, New Delhi 110025, India

## ARTICLE INFO

### Article history:

Received 24 December 2015

Received in revised form 5 March 2016

Accepted 8 March 2016

Available online 10 March 2016

### Keywords:

Sesamol

Acute toxicity

Comet assay

Micronucleus assay

Histopathology

Haematology

## ABSTRACT

The objective of this study was to evaluate organ-wise toxicological effects of sesamol and determine the LD<sub>50</sub> cut-off value and GHS category following acute oral toxicity method OECD 423. An acute oral toxicity study was carried out in female C57BL/6 mice. Observations for physical behaviour and measurements on haematology, biochemistry, histology of vital organs were performed. In addition, genotoxicity assessment using comet and micronuclei assays was also performed. Acute toxicological effects were observed at 2000 mg/kg, while no adverse effects observed at 300 mg/kg. The effects of 2000 mg/kg were manifested as severe histopathological changes in all organs (femur, spleen, gastrointestinal, lungs, heart, kidney, liver, stomach and brain) and excessive DNA strands breaks occurred in femoral bone marrow cells and splenocytes. A single dose of sesamol (2000 mg/kg, body weight) caused the death of two mice (out of three) within 2 h. Hence, sesamol is in GHS category 4 (>300–2000) with LD<sub>50</sub> cut-off value of 500 mg/kg body weight. In contrast, this study is correlated with the obtained GHS category 4 and LD<sub>50</sub> cut-off value 580 mg/kg body weight by ProTox. In conclusions, the present study has classified sesamol toxicity and assessed organ-wise acute oral toxicity of sesamol in female C57BL/6 mice. Therefore, these findings may be useful for the selection of dosages for further pre-clinical evaluation and potential drug developmental of sesamol.

© 2016 Published by Elsevier Ireland Ltd. This is an open access article under the CC BY-NC-ND license (<http://creativecommons.org/licenses/by-nc-nd/4.0/>).

## 1. Introduction

Oxidative stresses have been implicated as causative agents in various disorders such as hepatic fibrosis [34], pulmonary inflammation [33], cardio vascular disorders [8], diabetic complication [13], renal disease [3,38,42], cancer radiation syndrome [43], several neurodegenerative disorders [45] and the aging process [12]. Thus, antioxidants that scavenge free radicals and reactive oxygen species may be considerable potential in ameliorating these disease

processes. In the past few years, natural and endogenous antioxidants have created considerable research interest for prevention or amelioration of these diseases.

Sesamol (3,4-methylenedioxyphenol), is an important constituent of sesame oilseed and is well-known for its nutritional and medicinal value. It is used in ancient Chinese and Indian ayurvedic medicine for various health problems. The antioxidant properties have been attributed to a number of polyphenolic substances including sesamolin and sesamin [4]. Sesamol, possess good antioxidant activity due to a benzodioxole group, which is known to scavenge hydroxyl radical and also produces another antioxidant 1,2-dihydroxybenzene [23]. In a number of in-vitro and in-vivo investigations, sesamol has been documented as direct free radical scavenger and indirect antioxidant [17,18,32,35].

Sesamol is responsible for the stability of sesame oil [1], and is an efficacious potential antioxidant and free radical scavenger

\* Corresponding authors.

E-mail addresses: [shahanshah88@hotmail.com](mailto:shahanshah88@hotmail.com) (S. Khan), [pharmasan30@gmail.com](mailto:pharmasan30@gmail.com) (S. Choudhary), [arun.2k.64@gmail.com](mailto:arun.2k.64@gmail.com) (A. Kumar), [akanchha21tripathi@gmail.com](mailto:akanchha21tripathi@gmail.com) (A.M. Tripathi), [aalok.drdo@gmail.com](mailto:aalok.drdo@gmail.com) (A. Alok), [adhikari\\_56@yahoo.co.in](mailto:adhikari_56@yahoo.co.in) (J.S. Adhikari), [rizvi\\_ma@yahoo.com](mailto:rizvi_ma@yahoo.com) (M.A. Rizvi), [nkcinmas@rediffmail.com](mailto:nkcinmas@rediffmail.com), [nkchaudhury@gmail.com](mailto:nkchaudhury@gmail.com) (N.K. Chaudhury).

in comparison to many reference antioxidant molecules [27,28]. As a result of its marked stability sesame oil is used as vehicle for fat-soluble substances in pharmaceuticals and in food industry. In various in-vivo models, sesamol has shown some efficacy in different diseases such as pulmonary inflammation [6,7], anti-platelet [5], cardio vascular disorders, diabetes, diabetic nephropathy [22], renoprotective [14], hepatoprotective [41], cancer and mutagenesis [19], radioprotection [18,20,27,30,32,35,37], anticandidal [2], neurodegenerative disorders [39], and the anti-aging process [40]. Sesamol activates cAMP-PKA signaling, inhibits the NF-κB-PLC-PKC cascade thereby leading to inhibition of [Ca<sup>2+</sup>] immobilization and platelet aggregation. Therefore, sesamol appears to be having implications for treatment of cancer and various inflammatory diseases in addition to thromboembolic disorders [5].

Additionally, sesamol has properties to inhibit radiation induced micronuclei, dicentric frequencies, thiobarbituric acid reactive substances, DNA strands breaks [24] and also enhances glutathione (GSH), superoxide dismutase (SOD), catalase (CAT) and glutathione peroxidase (GPx) in a concentration dependent manner in irradiated cultured human lymphocytes [35]. Further, sesamol pre-treatment inhibits radiation-induced lymphocytes DNA strands breaks, lipid peroxidation and enhances the level of antioxidant enzymes (GSH, GST, catalase) to reduce lethality in irradiated mice [17,18,32]. In earlier studies, our research group has evaluated detailed antiradical properties of sesamol and found strong radical scavenging properties in comparison to other reference antioxidant molecules [27,28]. In addition, *in-vitro* studies using a V79 cell line, plasmid (pBR322) and calf thymus DNA, showed 20 times higher protection and greater DMF (dose modifying factor) than melatonin, possibly be due to its strong free radical scavenging property [27]. In continuation of these promising results, we have also reported that sesamol pre-treatment protects hematopoietic systems by reducing radiation-induced micronuclei frequencies, total chromosomal aberration and DNA strands breaks in mice bone marrow cells [24]. In another study, we have reported that sesamol pre-treatment protects hematopoietic system by reducing radiation-induced femoral hematopoietic progenitors stem cell depletion, and loss of B cells and T cells sub-population and apoptosis in the spleen [20]. In that study, we reported that sesamol pre-treatment protected the gastrointestinal system by enhancing crypt cell regeneration and inhibited lipid peroxidation, gut bacterial translocation to spleen, liver and kidney probably by controlling the expression pattern of p53, Bax and Bcl-x in irradiated mice [20]. These studies have revealed that sesamol is also a promising radioprotector candidate for medical and unanticipated radiation exposure.

Furthermore, bio-distribution and pharmacokinetics of sesamol has been reported and is shown to be distributed in all vital organs [16], desirable for making it a candidate for drug development for various disorders related to single or multi-organ systems. But, the lack of toxicity study is a major impediment for further development of this promising candidate for different applications. The objective of this study, therefore, was to investigate toxicity of sesamol as per the acute toxic class method, OECD-423 guideline in C57BL/6 female mice.

## 2. Materials and methods

### 2.1. Animal care and husbandry

Female C57BL/6 mice (8–10 week-old) weighing  $22 \pm 2$  g were randomly distributed divided into different groups and acclimatized for one week. Animals were housed in polypropylene cages containing certified paddy husk as bedding, and maintained on standard diet (Lipin, India) and acidified water *ad libitum* in the

animal house of the institute. The temperature and humidity were maintained at  $22 \pm 2^\circ\text{C}$  and 50% humidity under a 12-h light/dark cycles respectively. All protocols used in this experiment were approved by the Institutional Animal Ethics Committee. The Institutional Ethical Committee number under which this study was performed is INM/IEAC/2012/06. All efforts were made to minimize suffering during sacrifice of animal through cervical dislocation.

### 2.2. Experimental design

The mice were randomly divided into 4 groups, of 3 mice each as follows: Twelve-mice were divided randomly into four equal groups based on the OECD-423 guideline.

Group-I: Control group animals received no treatment.

Group-II: Sesamol 2000 group animals received 2000 mg/kg body weight of freshly prepared sesamol.

Group-III: Sesamol 300 group animals received 300 mg/kg body weight of freshly prepared sesamol.

Group-IV: Sesamol 300 confirmatory group animals received 300 mg/kg body weight of freshly prepared sesamol.

### 2.3. Sesamol preparation and administration

Sesamol (CAS No.: 533-31-3; Purity: 98%, Sigma-Aldrich, USA) was freshly prepared as a suspension in analytical grade water with 1% carboxymethylcellulose (CMC; Merck, Germany) as vehicle. A single dose of sesamol (either 300 or 2000 mg/kg) in a volume of 400 μl was administered orally using a canula (No. 16). The feed to mice was withheld, but not water for 3–4 h prior to sesamol administration. A starting dose of 2000 mg/kg was selected and orally administered to 3 mice (Group II) and observed for clinical signs and mortality. After observing the immediate deaths of all mice, a lower dose of 300 mg/kg body weight was administered to group III. When there were no signs of mortality observed, another 300 mg/kg dose was administered to group IV. Group I was administered with 400 μl vehicle as control.

### 2.4. Physical observation

The animals were closely observed for the first 30 min and intermittently for 4-h to 24-h, and then for 14 days after drug administration or until death for signs of acute toxicity, including convulsions, lacrimation, salivation, urination, defecation pain, distress, physical appearance and behavioural signs. The animals showing signs of severe toxicity were humanely sacrificed. Body weight was taken every day for 14 days.

### 2.5. Histopathological examination

To evaluate the toxicological alterations induced by sesamol in vital organs (femur, spleen, gastrointestinal, lungs, heart, kidney, liver, stomach and brain), mice were sacrificed by cervical dislocation and organs of interest were dissected out, cleaned in pre-chilled PBS and fixed in 10% formalin (v/v) at room temperature, as described earlier [21]. Briefly, five-micron thick sections were cut and placed on pre-cleaned slides. The sections were stained with haematoxylin and eosin (H & E), mounted and analyzed using an upright motorized compound microscope with DIC attached and a digital imaging system (Axio, Imager M2, Zeiss, Germany). Both the qualitative as well as quantitative (gastrointestinal) changes in organs were assessed. To avoid bias in analysis, all slides were independently coded before scoring and decoded after completion of analysis.

## 2.6. Biochemical analysis in blood plasma

Blood was collected through cardiac puncture using a 23-G needle with disposable 1 ml syringe into K<sub>2</sub>-EDTA vials (BD microtainer, San Diego, CA, USA). Plasma was separated by centrifugation at 2000g for 15 min in refrigerated centrifuge (4 °C) and stored at -80 °C. Biochemical parameters related to kidney (Urea and Creatinine) and liver (AST, ALT, LDH and TRIGS) function were analyzed following manufacturer's protocol (Randox, United Kingdom) using a biochemistry analyzer (Rx Monza, Randox, United Kingdom). All required calibration standards were performed before measurements.

## 2.7. Blood haematological analysis

Blood was collected by cardiac puncture using a 23-G needle and 1 ml disposable syringe, and about 100 µl blood was transferred into K<sub>2</sub>-EDTA vials (BD microtainer, San Diego, CA, USA) for haematology measurements. All haematological parameters (WBC, RBC, HGB, HCT, MCV, MCH, PLT, LY%, GR% RDW, PCT, MPV, PDW) measurements were made following manufacturer's protocol (NIHON-KOHDEN, Japan) using an automated haematology analyzer (Celtac-alpha, NIHON-KOHDEN, Japan). All required calibration standards were performed before measurement. The haematology analyzer was maintained in accordance with the external quality control of Randox.

## 2.8. Neutral comet assay in bone marrow and splenocytes

Femur and spleen was removed after cervical dislocation/death, cleaned of extra fat tissue and minced using frosted slides (for spleen) in petri dishes and flushed out bone marrow using a 26-G needle with syringe (for femur) in falcon tubes. Single cells suspensions were obtained by filtration with a 100 µM nylon mesh strainer (BD Biosciences, San Diego, CA, USA). In splenocytes, RBCs were lysed using lysis buffer (BD Biosciences, San Diego, CA, USA). The cell density ( $1 \times 10^6$  cells/ml) was assessed using a haemocytometer (Neubauer, Marienfeld, Germany) and inverted microscope (4200, Meiji, Japan).

A neutral comet assay was performed to assess the DNA strand breaks in bone marrow and splenocytes [31]. Briefly, single cell suspensions ( $4 \times 10^4$  cells) were mixed with 0.7% (w/v) low-melting-point agarose and immediately pipetted onto a pre-coated comet slide with 1% (w/v) normal-melting-point agarose. The slides were transferred onto slide tray resting on ice packs to harden the agarose layer (at least 10 min) and then immersed in a lysing solution (2.5% sodium dodecylsulfate, 1% sodium sarcosinate, 25 mM Na<sub>2</sub>EDTA, pH 9.5) containing 10% (v/v) DMSO for 15 min at RT. Further, slides were removed and placed side-by-side in a comet-20 system (Scie-Plas, Cambridge, England) fitted with a refrigerated water circulator (Julabo F12, Germany). The slides were immediately covered with freshly prepared neutral electrophoresis buffer (90 mM Trizma base, 90 mM Boric Acid, 2.5 mM Na<sub>2</sub>EDTA, pH 8.3) and electrophoresed (2 V/cm) using an electrophoresis power supply (Consort EV261, Belgium) for 7 min at 10 °C. After completion of electrophoresis, slides were washed with water and dried at 50 °C. When convenient, slides were stained with 2.5 µg/ml propidium iodide and at least 500 comet cells were scored for each mouse using an automated MetaCytte Comet Scan system (Metafer4, Zeiss, Germany).

## 2.9. Micronucleus assay in femoral bone marrow cells

Bone marrow cells were processed for micronuclei assessment from each mouse as described earlier [24]. Briefly, after washing the bone marrow cells were smeared on clean dry microscopic slide.

Slides were stained with cocktail of May–Grunewald and Giemsa solution. After staining the slides were mounted with DPX mounting solution and coded by independent person to avoid scorer bias in cell scoring. A minimum of 1000 polychromatic erythrocytes (PCE) were scored along with normochromatic erythrocytes (NCE) from each mouse to calculate the micronuclei frequency in both PCE and NCE. The ratio of PCE and NCE was also calculated to assess the status of cell proliferation. All cytogenetic slides were coded by a person not involved with this study and then analyzed. After completion of all analyses, slides were decoded.

## 2.10. Body and relative organ mass

Body weights of individual mouse were taken before and after fasting, and average body weight was used. Individual organs were excised and cleaned with cold PBS and weighed. The relative organ weights of individual mice were calculated as given below.

$$\text{Relative Organ Weight (ROW)} = \frac{\text{Organ Weight (mg)}}{\text{body Weight (g)}}.$$

## 2.11. In silico prediction of rodent oral toxicity

Acute oral toxicity of sesamol in rodent was predicted by Pro-Tox web server [9]. Sesamol toxicity was predicted as LD<sub>50</sub> (mg/kg) values and categorised by globally harmonized system of classification of labelling of chemicals (GHS). Pharmacophore search based sesamol similar compounds were identified having known LD<sub>50</sub>.

## 2.12. Statistical analysis

The mean values and standard errors of the data were analyzed and reported. Pairwise comparisons were made between two groups using Student's t-test. Significant differences among groups were considered if p < 0.05.

## 3. Results

### 3.1. Physical observations

The animals were observed for first 30 min and thereafter intermittently for 4 h to 24 h, and then daily for 14 days, after drug administration for signs of acute toxicity. The 2000 mg/kg dose group showed acute toxicity characterized by severe convulsions within 2–5 min of drug administration, with lacrimation, urination, wheezing sounds and apnoea leading to death. The first mouse died within 30 min of sesamol administration, other two mice were humanely sacrificed after similar signs of acute toxicity.

The C57BL/6 mice at 300 mg/kg showed slight jerking movement/convulsions with laboured breathing and rales, no signs of severe toxicity. All groups i.e., I, III, IV were observed daily for body weight changes, physical and behavioural signs such as: mucus from nostrils, laboured breathing, rales, vocalization on handling and aggressiveness. Such behavioural signs were absent in 300 mg/kg of sesamol treated mice. The animals were observed once daily for 14 days and no abnormal behaviour was observed other than vocalization and aggressiveness in 1–2 mice in groups III and IV on day 1 and 2. Body weights were recorded for 14 days, and no adverse changes were seen.

### 3.2. Determination of LD<sub>50</sub> cut-off value and classification according to GHS

A single dose of 2000 mg/kg of sesamol administered to three mice resulted in the death of all the three mice within 2-h after

administration. The next dose, 300 mg/kg, resulted in no deaths of mice within the period of 14 days observation. The confirmatory dose of 300 mg/kg of sesamol was also orally administered to three mice and resulted in no fatalities of mice within the period of 14 day observations. Therefore, sesamol was placed in GHS category IV (>300–2000) with LD<sub>50</sub> cut-off value of 500 mg/kg according to the OECD-423 guideline.

### 3.3. Gross histopathological changes in vital organs

Sesamol showed cellular toxicity in all organs examined at the higher dosage (2000 mg/kg). Both qualitative and quantitative (gastrointestine) analyses were performed to assess the level of cellular toxicity. Qualitative analysis revealed cellular toxicity (in terms of apoptosis, necrosis, depopulation and other parameters) in all major organs at higher dose (2000 mg/kg) (Figs. 1–9). The lower dose of sesamol (300 mg/kg) had no apparent effect on organ cellular toxicity (Fig. 1–9).

### 3.4. Toxicological effect of sesamol on bone marrow cellularity

Bone marrow is one of the largest organs in the body and is a major hematopoietic organ responsible for the production of erythrocytes, granulocytes, monocytes, lymphocytes and platelets [10]. Assessment of bone marrow, therefore, is frequently a routine procedure for the investigation of haematological disorders in toxicity and safety related studies. In addition, morphological assessment of bone marrow tissue sections provides information regarding their histological architecture such as cellularity, inflammation and necrosis. Thus, in the present study we have performed qualitative analysis of bone marrow. Sesamol group II (2000 mg/kg) indicated severe changes in the histological architecture, which were characterized by the severe loss of cellularity and extensive depopulation of lymphoid cells (Fig. 1C and D). While groups III and IV of sesamol (300 mg/kg) did not cause any changes in the bone marrow cellularity and revealed similar histological architecture of bone marrow in comparison to control (group I) (Fig. 1A and B).

### 3.5. Toxicological effects of sesamol on splenic histopathological alteration

Qualitative analysis in Group II of sesamol (2000 mg/kg) treated mice showed loss of cellularity and depopulation of lymphocytes, characterized by necrosis/apoptosis in lymphoid cells (Fig. 2C and D). The lower dose (300 mg/kg) showed no cellular toxicity (Fig. 2B) and appeared similar to control (Fig. 2A).

### 3.6. Histopathological alteration in gastrointestinal tract by sesamol

Both qualitative and quantitative analysis was performed to assess the effect of sesamol toxicity in epithelial stem cells. Analysis of sesamol group II (2000 mg/kg) treated mice showed extensive loss of epithelial stem cells and villi shrinking (Fig. 3C and D) resulting in significantly decreased crypts numbers and villi numbers and length (Fig. 3C and D). Normal histological architecture of gastrointestinal tract was observed in both the control and sesamol (300 mg/kg) treated mice (Fig. 3A). Quantitative analysis of gastrointestinal tissue also revealed and supported the extensive loss in the stem cell region of intestine, which were measured by counting the crypts and villi numbers. The data presented in Fig. 3D–F clearly show a significant decrease in the numbers of crypts and villi of 2000 mg/kg treated mice.

### 3.7. Sesamol-induced histopathological changes in stomach

The animals treated with the higher dose of sesamol (2000 mg/kg) revealed severe loss of gastric pits, isthmus and neck, base and extensive ruptured muscularis mucosa, such effect were completely absent in the lower dose of sesamol (300 mg/kg) treated mice (Fig. 4B–D).

### 3.8. Toxicological effect of sesamol on liver histology

Qualitative analysis of the liver of 2000 mg/kg treated mice showed swelling and degenerative changes followed by necrosis and dilated tubules (Fig. 5C and D), which were completely absent in 300 mg/kg treated mice (Fig. 5B).

### 3.9. Histopathological changes in kidney after sesamol treatment

The qualitative analysis of the kidneys of 2000 mg/kg treated mice showed swelling, focal degeneration and dilated tubules (Fig. 6C and D). Whereas, the kidneys of 300 mg/kg treated mice showed normal histological architecture of the glomerulus and Bowman's capsule (Fig. 6B).

### 3.10. Effect of sesamol treatment on the histology of the heart

The heart of control mice showed normal architecture of myocardial fibers (Fig. 7A). Extensive degeneration, fragmentation and hyalinization of myocardial fibers with congested blood vessel were observed in 2000 mg/kg treated mice, such effects were absent in 300 mg/kg treated mice (Fig. 7B).

### 3.11. Sesamol-induced histopathological alteration in lungs

The lung tissue of control mouse showed normal structure of alveoli with intra-alveolar septa (Fig. 8A). The lungs of mice treated with the higher dose of sesamol (2000 mg/kg) showed extensive emphysema and focal fibrosis of the alveoli with ruptured alveolar walls. In addition, haemorrhage with degeneration of alveoli was also detected in the higher dose of sesamol treated mice (Fig. 8C and D). Whereas, the lower dose of sesamol (300 mg/kg) revealed normal lungs and histological architecture, as showed in Fig. 8B.

### 3.12. Toxicological effects of sesamol on brain histology

In the brain of mice treated with the higher dose of sesamol (2000 mg/kg), severe neuronal degeneration followed by vacuolar changes was observed (Fig. 9C and D). The lower dose of sesamol (300 mg/kg) revealed a normal complexity of the brain similar to control (Fig. 9A and B).

### 3.13. Toxicological effects of sesamol on liver and kidney function

Urea and creatinine were measured to assess kidney function test (Fig. 10), whereas, AST, ALT, LDH and TRIGS were measured to assess the liver function test (Fig. 11).

#### 3.13.1. Biochemical test for liver function

Liver function test were conducted in sesamol 300 mg/kg and compared to control group and found to be similar. At 300 mg/kg and in the control group AST was 74 U/l and 71.80 U/l, respectively; though ALT was insignificantly increased ( $P > 0.05$ ) from 35.65 U/l in control to 47.55 U/l in 300 mg/kg group, and LDH activity was slightly decreased in 300 mg/kg group from 498.39 to 361.10 U/l ( $P > 0.05$ ). The level of triglycerides was significantly decreased (( $P < 0.05$ ) from 57.20 mg/dl in control to 30.30 mg/dl

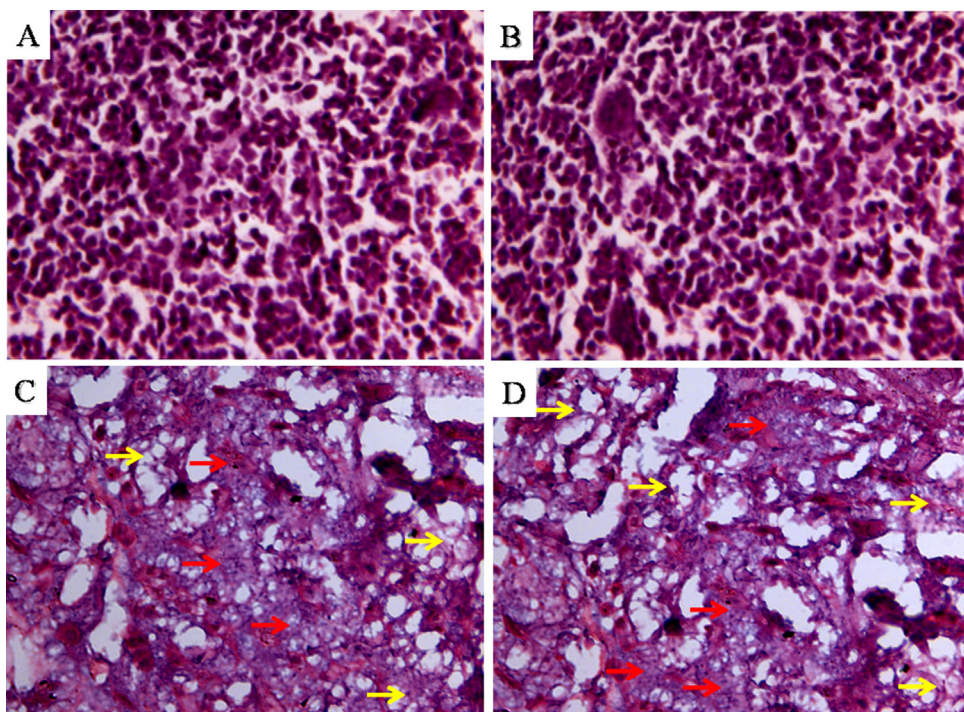


**Fig. 1.** Toxicological effect of sesamol in mice bone marrow cellularity. Femur was collected after cervical dislocation. After fixation, processing and dehydration, cross sections of femur ( $5\text{ }\mu\text{m}$ ) were stained with H&E. Representative photographs for femur are shown (original magnification and  $400\times$ ). Panel A: control, femur showing normal cellular architecture; Panel B: sesamol— $300\text{ mg/kg}$ , femur showing normal cellular architecture; Panel C and D: sesamol— $2000\text{ mg/kg}$ , femur showing extensive loss of cellularity (red arrow) and depopulation (yellow arrow) of the lymphoid cells. (Original magnification  $400\times$ ).

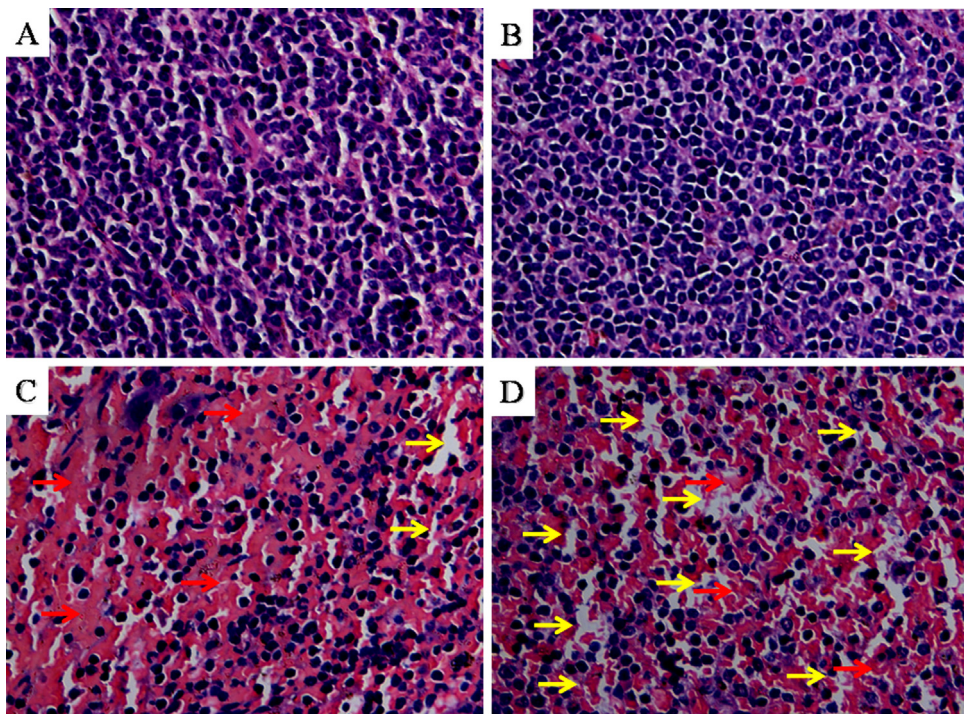


**Fig. 2.** Toxicological effects of sesamol in mice splenic histopathological alteration. Spleen was collected after cervical dislocation. After fixation, processing and dehydration, cross sections of jejunum ( $5\text{ }\mu\text{m}$ ) were stained with H&E. Representative photographs for spleen are shown (original magnification  $400\times$ ). Panel A: control, spleen showing normal cellular architecture; Panel B: sesamol— $300\text{ mg/kg}$ , spleen showing normal cellular architecture; Panel C and D: sesamol— $2000\text{ mg/kg}$ , spleen showing loss of cellularity (C) (red arrow) and depopulation (D) (yellow arrow) of the lymphocytes. (Original magnification  $400\times$ ).

in  $300\text{ mg/kg}$  group (Fig. 10). All the control values of measured parameters were in range similar to reported in literature [11] (Fig. 10).

### 3.13.2. Biochemical test for kidney function

In the  $300\text{ mg/kg}$  sesamol and control groups, urea was found to be  $30.70\text{ mg/dl}$  and  $29.00\text{ mg/dl}$ , respectively, whilst creatinine was insignificantly increased ( $P > 0.05$ ) from  $0.47\text{ mg/dl}$  in control

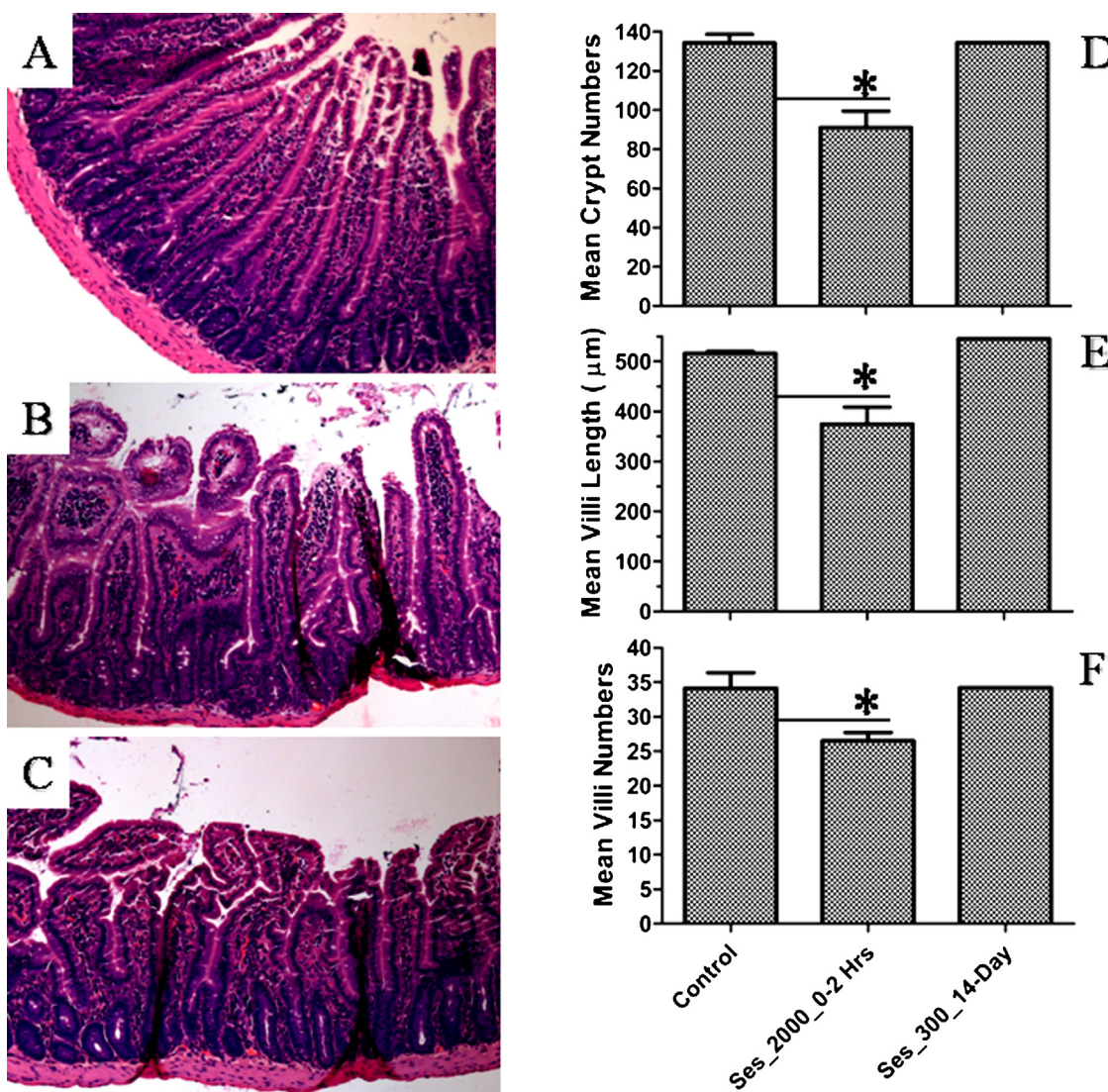


**Fig. 3.** Histopathological alteration in mice jejunum crypt number, villus number and length by sesamol treatment. Jejunum were collected after cervical dislocation. After fixation, processing and dehydration, cross sections of jejunum ( $5\text{ }\mu\text{m}$ ) were stained with H&E and crypt number, villus number and villus height were analyzed. Representative photographs for crypt number, villus number and villus height are shown (original magnification  $100\times$ ). Panel A: control/sesamol—300 mg/kg, showing normal gastrointestinal architecture; Panel C: sesamol—2000 mg/kg, showing ruptured villi tips and distorted villi and crypts. Panel D: comparison of mean crypt numbers between groups; Panel E: comparison of mean villi length between groups; Panel F: comparison of mean villi numbers between groups. \* $p < 0.05$ .

to 0.66 mg/dl in sesamol 300 mg/kg (Fig. 11). The control values of all parameters were found to be in range as reported earlier [11] (Fig. 11).

### 3.14. Toxicological effects of sesamol on blood haematological changes

The higher dose of sesamol (group II) significantly increased the blood parameters RBCs, HGB, HCT, LY%, MPV and decreased GR% in comparison to control (group I) (Table 1). Whereas, the lower dose of sesamol (group III and IV) did not cause any changes in the haematological parameters, and the values of haematological parameters were near to the corresponding control mice (group I) (Table 1).

### 3.15. Toxicological effects of sesamol on DNA strand breaks

The higher dose of sesamol group II (2000 mg/kg) was found to extensively increase DNA strands breaks parameters (tail

length, tail moment, olive moment and% DNA in tail) in both the marrow cells and spleenocyte in comparison to control (Figs. 12 and 13). Whereas, the lower dose of sesamol groups III and IV (300 mg/kg) did not cause DNA strands breaks; all DNA strands break parameters were similar to control mice (Figs. 12 and 13).

### 3.16. Toxicological effects of sesamol on the formation of micronuclei

The higher dose of Sesamol group II (2000 mg/kg) caused death within two hours, therefore, no micronuclei formation was observed. The result showed that frequency of mnPCE/1000 PCE ( $11.30 \pm 0.41$ ) in sesamol group II (2000 mg/kg) treated animals was almost similar to control mice (group I) ( $6.82 \pm 1.92$ ). The mnPCE frequency in sesamol group III & IV (300 mg/kg) treated animals ( $10.46 \pm 2.25$ ) was also near to control mice (group I) (Fig. 14).

The difference between frequencies of mnPCE in all the groups was non-significant ( $p > 0.05$ ). The proportion of immature (PCE)

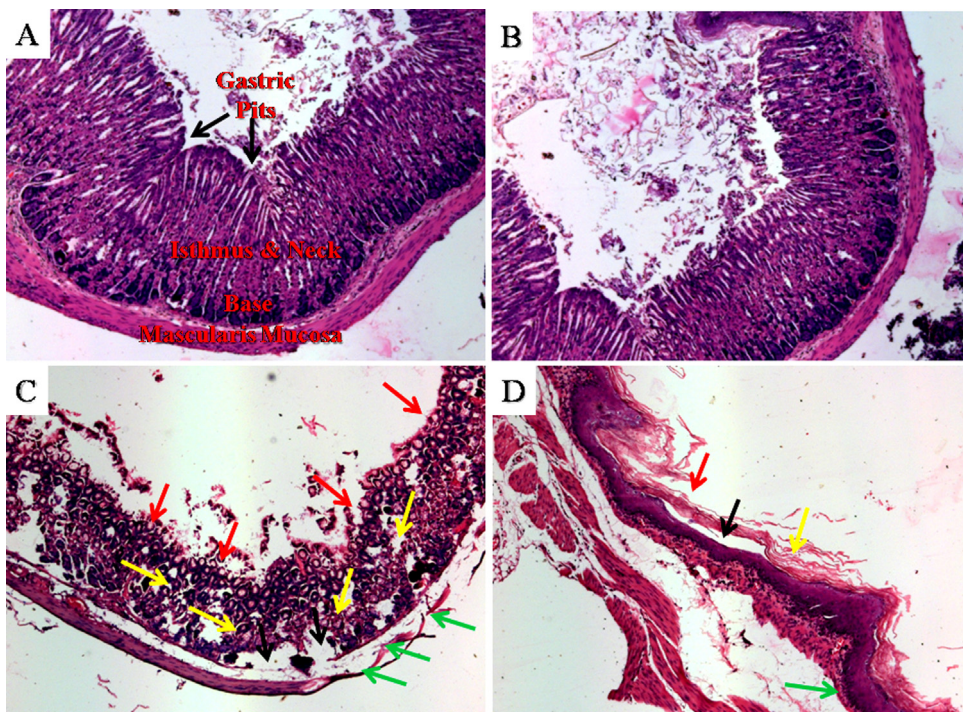


**Fig. 4.** Sesamol-induced histopathological changes in mice stomach. Stomach was collected after cervical dislocation. After fixation, processing and dehydration, cross sections of stomach ( $5\ \mu\text{m}$ ) were stained with H&E and gastric pits, isthmus and neck, base as well as muscularis mucosa were analyzed. Representative photographs for stomach are shown (original magnification  $100\times$ ). Panel A: control, stomach showing normal cellular architecture; Panel B: sesamol— $300\ \text{mg}/\text{kg}$ , stomach showing normal cellular architecture; Panel C and D: sesamol— $2000\ \text{mg}/\text{kg}$ , stomach showing almost complete loss of gastric pits (red arrow), isthmus and neck (yellow arrow), base (black arrow) and extensive ruptured muscularis mucosa (green arrow). (Original magnification  $100\times$ ).

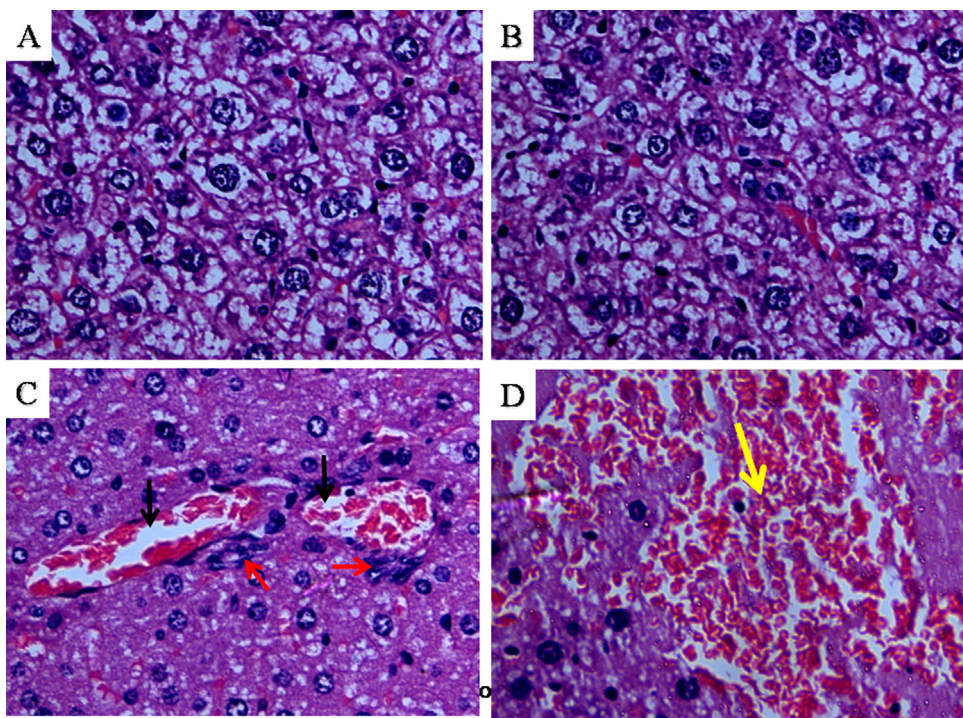


**Fig. 5.** Toxicological effect of sesamol in mice liver histology. Liver was collected after cervical dislocation. After fixation, processing and dehydration, cross sections of jejunum ( $5\ \mu\text{m}$ ) were stained with H&E. Representative photographs for liver are shown (original magnification  $400\times$ ). Panel A: normal. Liver showing normal histological architecture; Panel B: sesamol— $300\ \text{mg}/\text{kg}$ , liver showing normal histological architecture; Panel C and D: sesamol— $2000\ \text{mg}/\text{kg}$ , liver showing periportal lymphocytic infiltration (yellow arrow), necrotic hepatocytes near the central vein (red arrow), dilated central vein (black arrow). (original magnification  $400\times$ ).

along with mature (NCE) erythrocytes was determined to study the cellular toxicity and proliferation inhibition of bone marrow cell. The results showed that the PCE/NCE ratio was also not sig-

nificantly ( $p > 0.05$ ) different in all groups of sesamol treated mice (group II–IV) in comparison to control mice (group I) (Fig. 14). In the present study, therefore, the results suggest that neither the

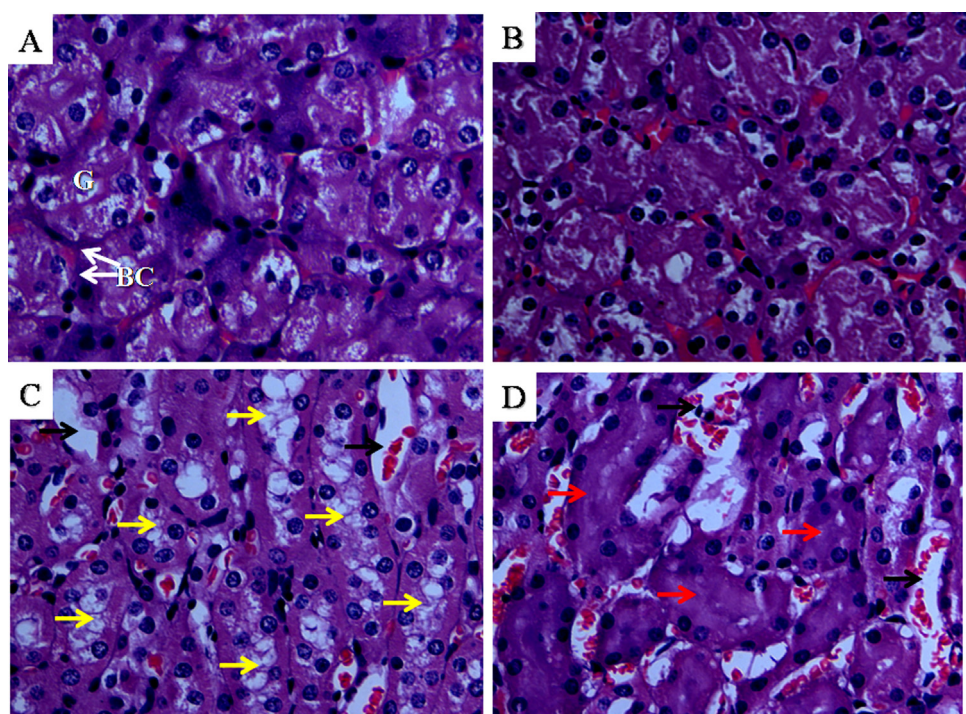


**Fig. 6.** Histopathological changes in mice kidney after sesamol treatment. Kidney was collected after cervical dislocation. After fixation, processing and dehydration, cross sections of jejunum ( $5\ \mu\text{m}$ ) were stained with H&E. Representative photographs for kidney are shown (original magnification  $400\times$ ). Panel A: Normal. Kidney showing normal histological architecture of renal corpuscles with its glomerulus (G) and Bowman's capsule (BC); Panel B: sesamol— $300\ \text{mg}/\text{kg}$ , kidney showing normal histological architecture; Panel C and D: sesamol— $2000\ \text{mg}/\text{kg}$ , kidney showing swelling (red arrow), focal degeneration (yellow arrow) and dilated tubules (black arrow). (Original magnification  $400\times$ ).

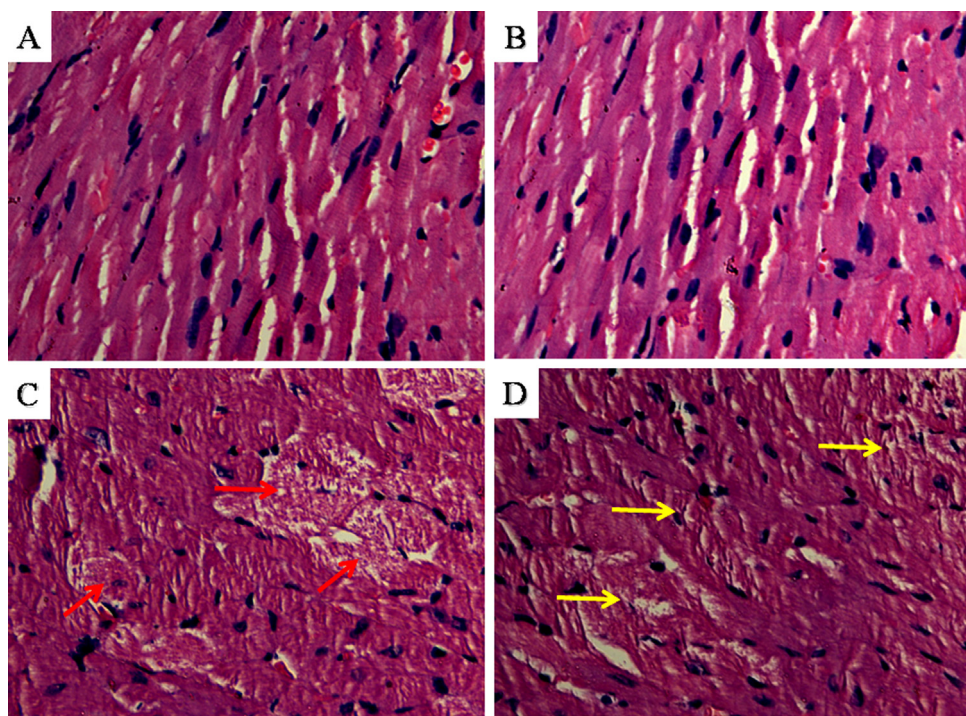


**Fig. 7.** Effect of sesamol treatment in histology of mice heart. Heart was collected after cervical dislocation. After fixation, processing and dehydration, cross sections of heart ( $5\ \mu\text{m}$ ) were stained with H&E. Representative photographs for heart are shown (original magnification  $400\times$ ). Panel A: Normal. Heart showing normal histological architecture; Panel B: sesamol— $300\ \text{mg}/\text{kg}$ , heart showing normal histological architecture; Panel C and D: sesamol— $2000\ \text{mg}/\text{kg}$ , heart showing extensive degeneration, fragmentation and hyalinization of muscle fibers (H) with congested blood vessel (red arrow). (original magnification  $400\times$ ).

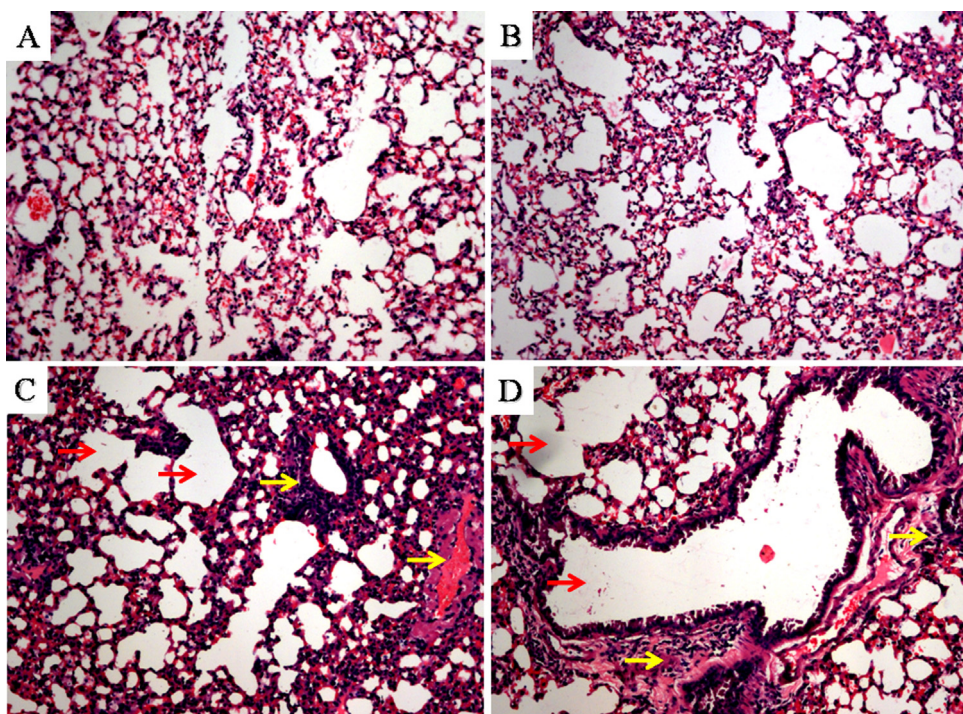


**Fig. 8.** Sesamol-induced histopathological alteration in mice lungs. Lung was collected after cervical dislocation. After fixation, processing and dehydration, cross sections of lung ( $5\ \mu\text{m}$ ) were stained with H&E. Representative photographs for lung are shown (original magnification  $100\times$ ). Panel A: Control, lung showing normal cellular architecture; Panel B: Sesamol— $300\ \text{mg}/\text{kg}$ , lung showing normal cellular architecture; Panel C and D: Sesamol— $2000\ \text{mg}/\text{kg}$ , lung showing extensive emphysema and focal fibrosis of the alveoli with ruptured alveolar walls (red arrow), and haemorrhage with degeneration of alveoli (yellow arrow). (Original magnification  $100\times$ ).

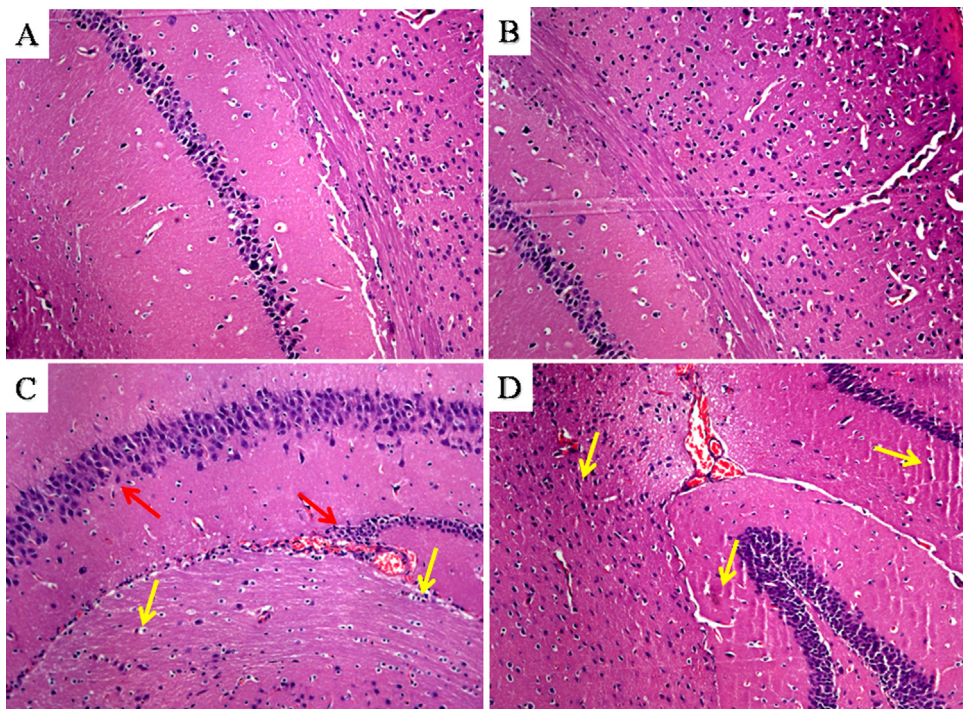


**Fig. 9.** Toxicological effects of sesamol in mice brain histology. Brain was collected after cervical dislocation. After fixation, processing and dehydration, cross sections of brain ( $5\ \mu\text{m}$ ) were stained with H&E. Representative photographs for brain are shown (original magnification  $100\times$ ). Panel A: Control, brain showing normal cellular architecture; Panel B: sesamol— $300\ \text{mg}/\text{kg}$ , brain showing normal cellular architecture; Panel C and D: sesamol— $2000\ \text{mg}/\text{kg}$ , brain showing severe neuronal degeneration (red arrow) and vacuolar changes (yellow arrow). (Original magnification  $100\times$ ).

higher dose of sesamol  $2000\ \text{mg}/\text{kg}$  (group II) nor lower dose of sesamol  $300\ \text{mg}/\text{kg}$  (group III and IV) was able to induce formation of micronuclei in bone marrow cells.

### 3.17. Toxicological effects of sesamol in relative organ weight

The higher dose of sesamol ( $2000\ \text{mg}/\text{kg}$ ) did not cause any significant changes in spleen, lungs, heart, kidney, stomach and brain

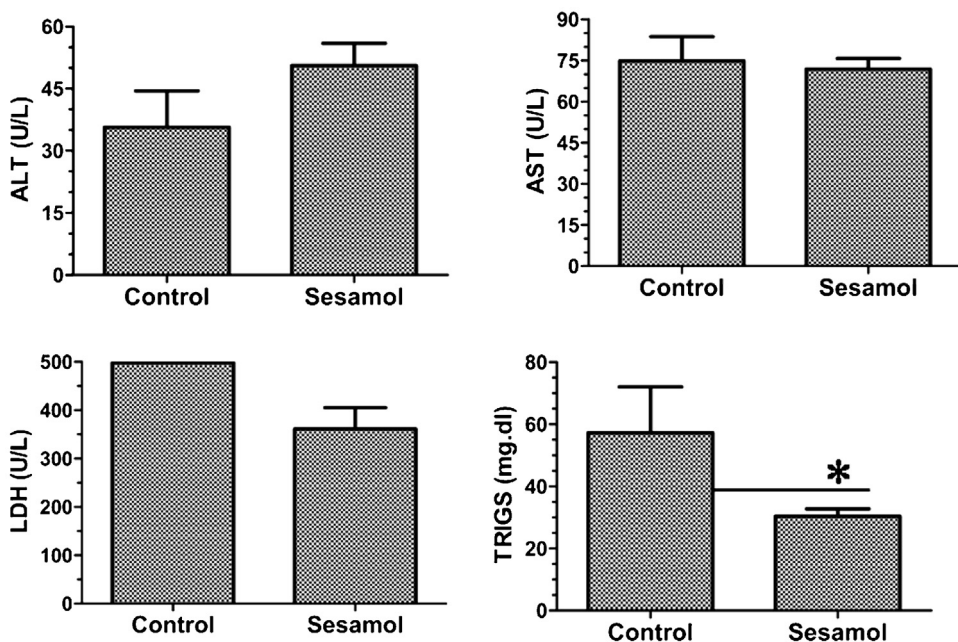


**Fig. 10.** Effect of sesamol (300 mg/kg body weight) on liver function. AST, ALT, LDH and TRIGS were measured in blood plasma as described in materials and methodology. \* $p < 0.05$ .

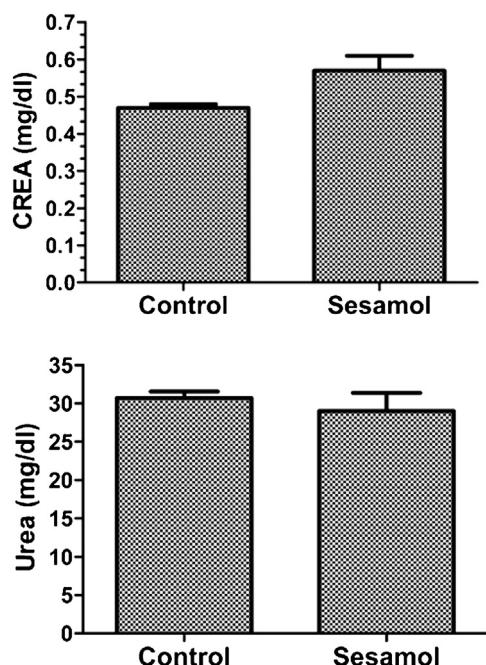


**Fig. 11.** Effect of sesamol (300 mg/kg body weight) on kidney function. Urea and creatinine were measured in blood plasma as described in materials and methodology.

(except liver) in comparison to control (Fig. 15). The lower dose of sesamol (300 mg/kg) value was similar to control mice (Fig. 15).

### 3.18. In silico prediction of sesamol oral toxicity in rodent

Sesamol can be placed under class 4 category and predicted LD<sub>50</sub> dose was found to be 580 mg/kg body weight. The LD<sub>50</sub> value revealed that sesamol would be harmful if swallowed ( $300 < \text{LD}_{50} \leq 2000$  mg/kg). Based on pharmacophore search the average similarity and prediction accuracy of sesamol are 76.07%

and 69.26%, respectively. However, three compounds similar to sesamol were identified (Table 2).

## 4. Discussion

Herbal derived medicines are gaining importance, it is therefore necessary to establish safety, toxicity, and efficacy and quality data in accordance with regulatory guideline. Sesamol has already shown efficacy in various preclinical models, and appeared to be a potential drug candidate [17,18,32,35,24,20]. Toxicity studies on sesamol have not been extensively studied in accordance to internationally recognized OECD guidelines. In the present study we have investigated the toxicity of sesamol in female C57BL/6 mice following the OECD-423 guideline. The study presented here considers the GHS classification of sesamol as a GHS 4 category molecule.

Ambrose et al. [1], conducted toxicological studies with rodents, non-human primates and human volunteers, and demonstrated that sesamol was non-irritant to the skin and did not cause skin sensitization. This study made several observations, (i) injection of aqueous solution equivalent to 5 mg/kg of sesamol through the intra-dermal route developed necrosis at the site of injection within 4 days in six rats out of ten, (ii) injection of aqueous solution equivalent to 50 mg/kg through intra-dermal route for 4 days in three rabbits did not cause local or systemic effects, (iii) sesamol doses of 1.2, 2.3 and 4.6 mg/kg was administered to six rabbit each dose in the conjunctiva sac and found oedema of the nictitating membrane, swelling of the palpebral folds and conjunctivitis within 4-h, whereas, relatively all mice appeared near to normal after 48-h. Ambrose et al. also reported forestomach tumours due to chronic administration of sesamol. In addition, consolidation and inflammatory changes were observed in lungs [1]. In the present study, physical observation as congestive atelectasis and histopathological changes in lungs revealed an acute inflammatory infiltrate, and decreased PCV in haematological measurements and therefore can be correlated with the acute effects in respiratory system.

In this study, we have found a higher dose of sesamol (2000 mg/kg) induced severe histopathological changes in all vital organs, which were characterized by (i) loss of cellularity and

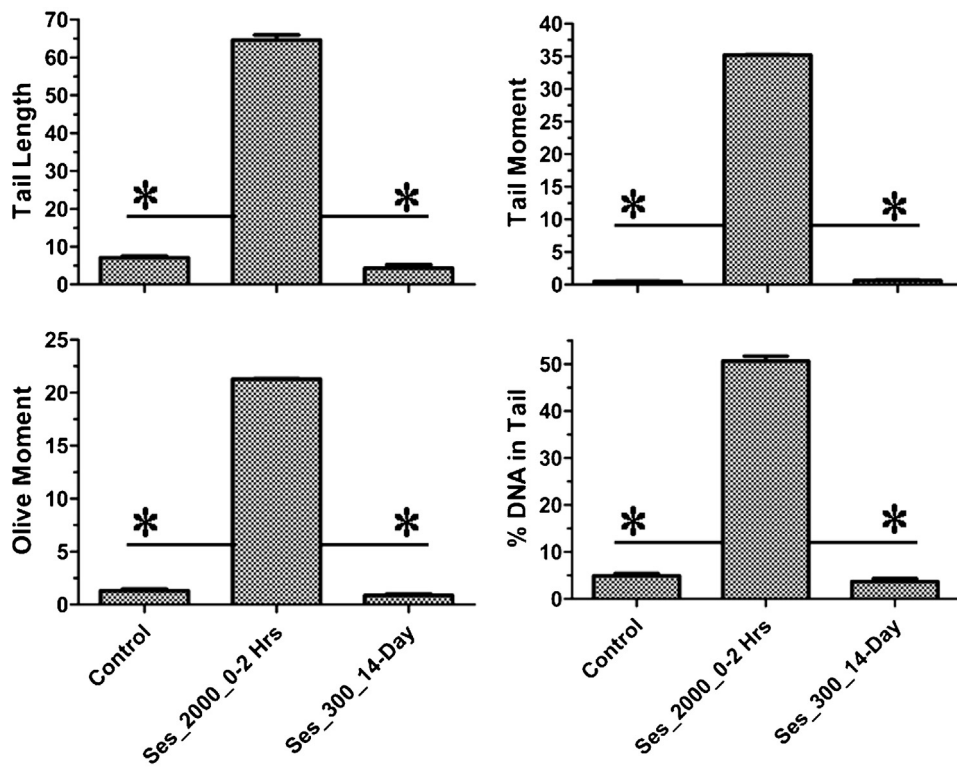


**Fig. 12.** Effect of sesamol on DNA double strands breaks in femoral bone marrow of mice. A neutral comet assay was performed to analyzed DNA strands breaks as described in materials and methodology. DNA strands breaks are represented as tail length, tail moment, olive moment and% DNA in tail. \* $p < 0.001$ .

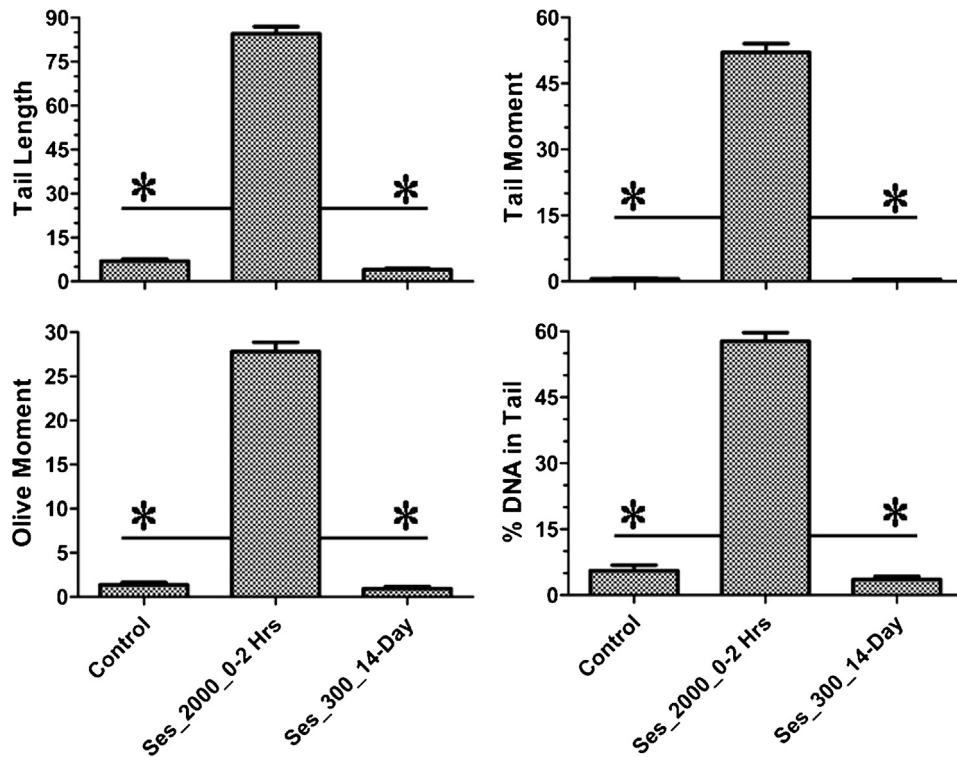


**Fig. 13.** Effect of sesamol on DNA double strands breaks in splenocytes of mice. A neutral comet assay was performed to analyzed DNA strands breaks as described in materials and methodology. DNA strands breaks are represented as tail length, tail moment, olive moment and% DNA in tail. \* $p < 0.0001$ .

extensive depopulation of lymphoid cells in femur (ii) necrosis/apoptosis of lymphoid cells in spleen, (iii) extensive loss of epithelial stem cells and villi shrinking in gastrointestinal, (iv)

severe loss of gastric pits, isthmus and neck, base as well as extensive ruptured muscularis mucosa in stomach, (v) swelling, degeneration, necrosis and dilated tubules in liver, (vi) swelling,

**Table 1**  
Sesamol-mediated haematological modulation.

Groups	Statistics	Haematological Parameters											
		WBC ( $10^3/\mu\text{l}$ )	RBC ( $10^6/\mu\text{l}$ )	HGB (g/dl)	HCT (%)	MCV (fl)	MCH (pg)	MCHC (g/dl)	PLT ( $10^3/\mu\text{l}$ )	LY (%)	GR (%)	RDW (%)	PCT (%)
Control	Mean	5.37	8.81	12.77	40.03	45.5	14.5	31.75	782.67	73.47	26.53	13.5	0.27
	SD	0.65	0.58	0.47	1.44	1.51	0.53	0.21	19.04	3.27	3.27	0.1	0.01
Ses_2000_0–2h	Mean	6	10.5 <sup>a</sup>	15.8 <sup>a</sup>	49.33 <sup>b</sup>	46.83	15	31.7	805	80.57 <sup>b</sup>	19.43 <sup>b</sup>	13.57	0.27
	SD	2.07	0.17	0.35	0.58	1.19	0.4	0.42	66.47	3.44	3.44	0.12	0.1
Ses_300_14 day	Mean	4.88	9.07	13.62	41.6	45.9	15.02	32.72	767	72.25	27.68	13.82	0.27
	SD	1.16	0.23	0.26	0.85	0.87	0.42	0.4	150.08	3.58	3.1	0.46	0.04

Statistical significant difference between Control and Sesamol 2000 mg/kg body weight groups.

<sup>a</sup>  $P < 0.05$ .

<sup>b</sup>  $P < 0.01$ .

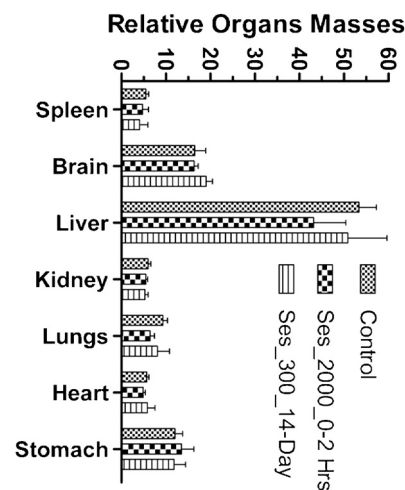
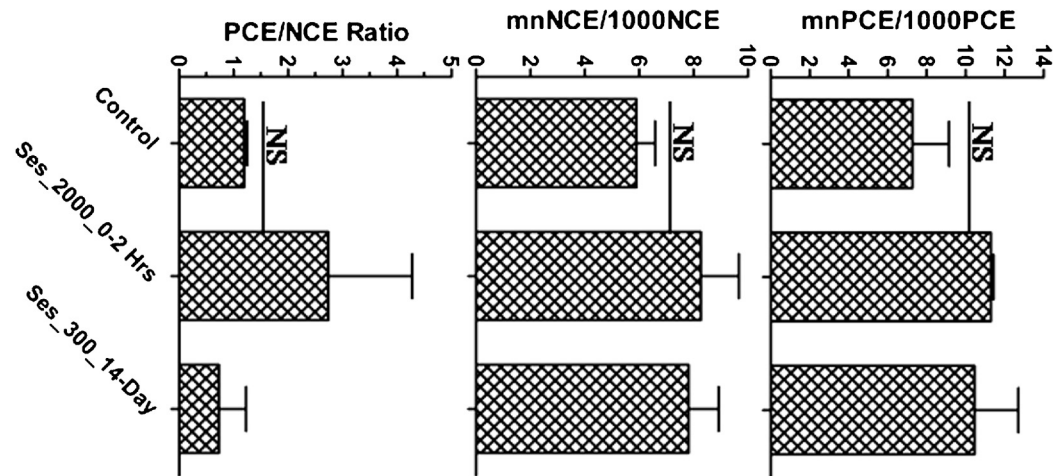


**Fig. 15.** Effect of sesamol on relative organ masses. Each organ was weighed after removing extra tissues. The ROM was determined by dividing the organ mass (mg) with body mass (g).

**Fig. 14.** Effect of sesamol on the formation of micronuclei in bone marrow cells. Micronuclei Assay was performed in bone marrow cells to analyze the cytogenetic effects of sesamol on DNA as described in materials and methodology. NS=non significant.



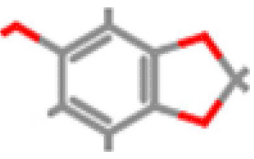
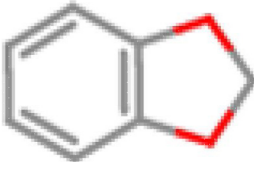
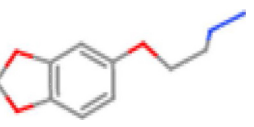
focal degeneration and dilated tubules in kidney, (vii) extensive degeneration, fragmentation and hyalinization of myocardial fibers with congested blood vessel in heart, (viii) extensive emphysema and focal fibrosis of the alveoli with ruptured alveolar walls as well as haemorrhage with degeneration of alveoli in lung, (ix) severe neuronal degeneration followed by vacuolar changes in brain (Figs. 1–9).

Induction of DNA damage is considered as one of the important initial event in cellular toxicity. It is also well known that mechanisms of cellular toxicity involve DNA damage. The comet assay is a sensitive method for detecting cellular DNA damage. In this study, we have used the comet assay to assess the femoral bone marrow cells and splenocytes cellular DNA damage after sesamol treatment. We have found that sesamol induced extensive DNA damage in 2000 mg/kg group within the 2 h in comparison to control group (Figs. 12 and 13). Whilst, the sesamol 300 mg/kg group showed DNA damage close to control group (Figs. 12 and 13). On the other hand, no such genotoxicity was observed using a micronucleus assay with sesamol at 2000 mg/kg (Fig. 14). The comet assay findings together with histopathological observation in the femur and spleen suggests that higher dose of sesamol (2000 mg/kg) appeared to be very toxic at the level of DNA. The comet assay findings also demonstrated that lower dose of sesamol (300 mg/kg) induced no apparent effects on DNA (Figs. 12 and 13).

In addition, biochemical markers related to kidney (urea and creatinine) and liver (AST, ALT, LDH and TRIGS) function were measured in the sesamol (300 mg/kg) group and compared with control groups, similar results were seen (Figs. 10 and 11). Plasma amino transferases such as ALT and AST indicate the concentration of hepatic intracellular enzymes that have leaked into the circulation as a result of hepatocellular injury [15]. In this study, level of AST in 300 mg/kg group was comparable to normal control, while ALT was insignificantly increased ( $P > 0.05$ ), indicative of possibly low hepatotoxicity. LDH activity was slightly decreased ( $P > 0.05$ ) in 300 mg/kg group, which may indicate possibly low level of liver insult. TRIGS were found to decrease significantly ( $p < 0.05$ ) in the sesamol 300 mg/kg group in comparison to control group. This was expected (i.e., decrease of TRIGS) because inhibition of cholesterol biosynthesis and increase of uptake of LDL from blood by sesamol contained in sesamol oil, has been reported [36]. In case of deterioration of kidney function, urea and creatinine levels always increases in combination. In our study the levels were similar to control, suggesting that kidney function was not affected by administration of the sesamol.

In order to assess toxicological effects of sesamol on blood parameters a complete blood haematological measurements were performed in mice treated with sesamol (group II–IV) and compared with control mice (group I). Analysis of data revealed that only sesamol group II (2000 mg/kg) has significantly altered the

**Table 2**  
ProTox predicted sesamol similar compounds.

Sesamol	Sesamol similar compounds		
	Compound 1	Compound 2	Compound 3
			
Formula	$C_7H_6O_3$	Formula	$C_{15}H_{22}O_6$
Molecular Weight	138.12	Molecular Weight	298.33
Toxicity Class	4	Toxicity Class	4
LD50	580 mg/kg	LD50	580 mg/kg

**Table 3**  
Physio-chemical properties of sesamol.

Sl No.	Physio-Chemical Properties	Sesamol
1	IUPAC	1,3-benzodioxol-5-ol
2	CAS No.	533-31-3
3	Formula	$C_7H_6O_3$
4	Synonyms	Phenol,3,4-(methylenedioxy)-(7CI,8CI); 3,4-(Methylenedioxy) phenol; 4-Hydroxy1,2-methylenedioxybenzene; 5-Hydroxy-1,3-benzodioxole; Benzodioxol-5-ol;NSC59256; 3,4-Methylenedioxyphenol
5	Appearance	white to off-white crystalline
6	Molecular Weight	138.12 g/mol
7	Melting Point	6265 °C (l)
8	Boiling point	274 °C at 760 mmHg
9	Storage Temperature	20 °C
10	Flash Point	119.5 °C
11	Density	1.394 g/cm <sup>3</sup>
12	Water Solubility	slightly soluble
13	Refraction Index	1.609
14	Molar Refractivity	34.29 cm <sup>3</sup>
15	Molar Volume	99 cm <sup>3</sup>
16	Surface Tension	61.7 dyn/cm
17	Vaporization Enthalpy	53.3 kJ/mol
18	Vapour Pressure	0.00331 mmHg at 25 °C
19	Lipophilicity (LogP)	1.2
20	H-Bond Donor	1
21	H-Bond Acceptor	3

**Table 4**  
Sesamol's Lipinski rule of five.

Sl. No.	Lipinski Rule of Five	Sesamol
1	Molecular mass (less than 500 Da)	138.121 g/mol
2	High lipophilicity (LogP less than 5)	1.121
3	Donors hydrogen bond (Less than 5)	1
4	Acceptors hydrogen bond (Less than 10)	3
5	Molar refractivity (Between 40–130)	34.29 cm <sup>3</sup>

level of RBCs, HGB, HCT, MPV, LY% and GR% (Table 1). The increased value of RBCs, HGB, HCT, LY% and MPV indicates drug toxicity which could be because of apnea or pulmonary fibrosis or due to polycythemia [44]. The apnea was also observed as physical parameter while monitoring the mice. Polycythemia is an apparent rise of the erythrocyte level in the blood which may be caused by reduced blood plasma. Relative polycythemia is often caused by loss of body fluids, such as through dehydration and stress which may be caused by 2000 mg/kg of sesamol (group II). The sesamol induced increase in some of the haematological parameters is in accordance with the toxicological studies [44]. The increase in PCV, HGB and RBCs reported in this study to be associated with sesamol injec-

tion may be attributed to the reversal of bone marrow depression with attendant improvement in erythrocyte membrane stability. Moreover, sesamol has strong antioxidant properties and these antioxidant properties attributes to reduced haemolysis. However, femur has shown severe loss of cellularity in the histological studies despite that there was an increase in haematological parameters. The reason could be that mice were sacrificed between 30 min to 2 h interval and the effect of bone marrow depletion could not impact the haematological outcome within 2 h [26,29].

ProTox; web server predicted sesamol GHS category 4 and LD<sub>50</sub> cut-off value 580 mg/kg body weight in rodent [9] (Table 2). This study is correlated with the obtained GHS category 4 and LD<sub>50</sub> cut-off value 500 mg/kg body weight by following acute oral toxicity method (OECD 423 guideline) in female C57BL/6 mice. Thus, both in-vivo and in-silico studies provided similar acute oral toxicity of sesamol in rodent. In addition, we have also mentioned the sesamol physico-chemical properties (Table 3). The sesamol almost follow the Lipinski rule of five (Table 4) [25]. The drugs that follow the Lipinski rule of five are likely to have decreased attrition during clinical trials.

## 5. Conclusions

This study was conducted in accordance with the OECD-423 guideline. From the observations in the present study, sesamol should be placed under GHS category 4 (>300–2000) with LD<sub>50</sub> cut-off value of 500 mg/kg in female C57BL/6 mice. This study also demonstrated clear toxicological effects, biochemical changes and genomics alterations induced by sesamol in female C57BL/6 mice. These findings could, therefore, can be helpful for the selection of dosages for pre-clinical in murine models and for additional studies on sesamol in the drug developmental process. Further, toxicity studies and their validation using others animal models may be warranted.

## Acknowledgements

Shahanshah Khan is grateful to Director, INMAS, Delhi, for providing work facility. Authors are also grateful to Dr. B G Roy for necessary animal facility and Dr I Namita for haematological and biochemical measurement at INMAS. This work was supported by the Defence Research & Development Organization at Institute of Nuclear Medicine and Allied Sciences (INMAS), project on "Development of Safe Chemical Radioprotector" (NBC 1.29).

## References

- [1] A.M. Ambrose, A.J. CoxJr, F. DeEds, Antioxidant toxicity, toxicological studies on sesamol, *J. Agric. Food Chem.* 6 (1958) 600–604.
- [2] M.A. Ansari, Z. Fatima, S. Hameed, Sesamol: a natural phenolic compound with promising anticandidal potential, *J. Pathog.* 2014 (2014) 895193.
- [3] E.I. Azzam, J.P. Jay-Gerin, D. Pain, Ionizing radiation-induced metabolic oxidative stress and prolonged cell injury, *Cancer Lett.* 327 (2012) 48–60.
- [4] P. Budowski, K.S. Markley, The chemical and physiological properties of sesame oil, *Chem. Rev.* 48 (1951) 125–151.
- [5] C.C. Chang, W.J. Lu, E.T. Ong, C.W. Chiang, S.C. Lin, S.Y. Huang, J.R. Sheu, A novel role of sesamol in inhibiting NF- $\kappa$ B-mediated signaling in platelet activation, *J. Biomed. Sci.* 18 (2011) 93.
- [6] P.Y. Chu, S.P. Chien, D.Z. Hsu, M.Y. Liu, Protective effect of sesamol on the pulmonary inflammatory response and lung injury in endotoxicemic rats, *Food Chem. Toxicol.* 48 (2010) 1821–1826.
- [7] P.Y. Chu, D.Z. Hsu, P.Y. Hsu, M.Y. Liu, Sesamol down-regulates the lipopolysaccharide-induced inflammatory response by inhibiting nuclear factor- $\kappa$ B activation, *Innate Immun.* 16 (2010) 333–339.
- [8] N.S. Dhalla, R.M. Temsah, T. Netticadan, Role of oxidative stress in cardiovascular diseases, *J. Hypertens.* 18 (2000) 655–673.
- [9] M.N. Drwal, P. Banerjee, M. Dunkel, M.R. Wetzig, R. Preissner, ProTox: a web server for the *in silico* prediction of rodent oral toxicity, *Nucleic Acids Res.* 42 (2014) W53–58.
- [10] B.F. Feldman, J.G. Zinkl, N.C. Jain, P.E. Gasper, U. Giger, R.R. De Gopegui, C.B. Grindem, A.T. Kristensen, K.S. Latimer, K. Rogers, Schalm's Veterinary Hematology, Wiley, 2000.
- [11] I. Fernandez, A. Pena, N. Del Teso, V. Perez, J. Rodriguez-Cuesta, Clinical biochemistry parameters in C57BL/6J mice after blood collection from the submandibular vein and retroorbital plexus, *J. Am. Assoc. Lab. Anim. Sci.* 49 (2010) 202–206.
- [12] T. Finkel, N.J. Holbrook, Oxidants, oxidative stress and the biology of ageing, *Nature* 408 (2000) 239–247.
- [13] F. Giacco, M. Brownlee, Oxidative stress and diabetic complications, *Circ. Res.* 107 (2010) 1058–1070.
- [14] A. Gupta, S. Sharma, I. Kaur, K. Chopra, Renoprotective effects of sesamol in ferric nitrilotriacetate-induced oxidative renal injury in rats, *Basic Clin. Pharmacol. Toxicol.* 104 (2009) 316–321.
- [15] N. Han, H.K.S. Htoo, H. Aung, Determinants of abnormal liver function tests in diabetes patients in Myanmar, *Int. J. Diab. Res.* 1 (2012) 36–41.
- [16] K.C. Jan, C.T. Ho, L.S. Hwang, Bioavailability and tissue distribution of sesamol in rat, *J. Agric. Food Chem.* 56 (2008) 7032–7037.
- [17] R. Joshi, M.S. Kumar, K. Satyamoorthy, M.K. Unnikrishnan, T. Mukherjee, Free radical reactions and antioxidant activities of sesamol: pulse radiolytic and biochemical studies, *J. Agric. Food Chem.* 53 (2005) 2696–2703.
- [18] P. Kanimozi, N.R. Prasad, Antioxidant potential of sesamol and its role on radiation-induced DNA damage in whole-body irradiated Swiss albino mice, *Environ. Toxicol. Pharmacol.* 28 (2009) 192–197.
- [19] I.P. Kaur, A. Saini, Sesamol exhibits antimutagenic activity against oxygen species mediated mutagenicity, *Mutat. Res.* 470 (2000) 71–76.
- [20] S. Khan, A. Kumar, J.S. Adhikari, M.A. Rizvi, N.K. Chaudhury, Protective effect of sesamol against  $^{60}$ Co  $\gamma$ -ray-induced hematopoietic and gastrointestinal injury in C57BL/6 male mice, *Free Radic. Res.* 49 (2015) 1344–1361.
- [21] S. Khan, J.S. Adhikari, M.A. Rizvi, N.K. Chaudhury, Radioprotective potential of melatonin against  $^{60}$ Co  $\gamma$ -ray-induced testicular injury in male C57BL/6 mice, *J. Biomed. Sci.* 22 (2015) 1–15.
- [22] A. Kuhad, A.K. Sachdeva, K. Chopra, Attenuation of renoinflammatory cascade in experimental model of diabetic nephropathy by sesamol, *J. Agric. Food Chem.* 57 (2009) 6123–6128.
- [23] Y. Kumagai, L.Y. Lin, D.A. Schmitz, A.K. Cho, Hydroxyl radical mediated demethylation of (methyleneoxy) phenyl compounds, *Chem. Res. Toxicol.* 4 (1991) 330–334.
- [24] A. Kumar, T.G. Selvan, A.M. Tripathi, S. Choudhary, S. Khan, J.S. Adhikari, N.K. Chaudhury, Sesamol attenuates genotoxicity in bone marrow cells of whole-body gamma-irradiated mice, *Mutagenesis* 30 (2015) 651–661.
- [25] P. Leeson, Drug discovery: chemical beauty contest, *Nature* 481 (2012) 455–456.
- [26] L.K. Mahan, S. Escott-Stump, Krause's Food, Nutrition, & Diet Therapy, Saunders, 2004.
- [27] K. Mishra, P.S. Srivastava, N.K. Chaudhury, Sesamol as a potential radioprotective agent: in vitro studies, *Radiat. Res.* 176 (2011) 613–623.
- [28] K. Mishra, H. Ojha, N.K. Chaudhury, Estimation of antiradical properties of antioxidants using DPPH assay: a critical review and results, *Food Chem.* 130 (2012) 1036–1043.
- [29] F. Naaz, S. Javed, M.Z. Abdin, Hepatoprotective effect of ethanolic extract of *Phyllanthus amarus* Schum. et Thonn: on aflatoxin B1-induced liver damage in mice, *J. Ethnopharmacol.* 113 (2007) 503–509.
- [30] G.G. Nair, C.K. Nair, Protection of cellular DNA and membrane from gamma-radiation-induced damages and enhancement in DNA repair by sesamol, *Cancer Biothe. Radiopharm.* 25 (2010) 629–635.
- [31] O. Ostling, K.J. Johanson, Microelectrophoretic study of radiation-induced DNA damages in individual mammalian cells, *Biochem. Biophys. Res. Commun.* 123 (1984) 291–298.
- [32] V.K. Parihar, K.R. Prabhakar, V.P. Veerapur, M.S. Kumar, Y.R. Reddy, R. Joshi, M.K. Unnikrishnan, C.M. Rao, Effect of sesamol on radiation-induced cytotoxicity in Swiss albino mice, *Mutat. Res.* 611 (2006) 9–16.
- [33] H.S. Park, S.R. Kim, Y.C. Lee, Impact of oxidative stress on lung diseases, *Respirology* 14 (2009) 27–38.
- [34] G. Poli, Pathogenesis of liver fibrosis: role of oxidative stress, *Mol. Aspects Med.* 21 (2000) 49–98.
- [35] N.R. Prasad, V.P. Menon, V. Vasudev, K.V. Pugalendi, Radioprotective effect of sesamol on gamma-radiation induced DNA damage, lipid peroxidation and antioxidants levels in cultured human lymphocytes, *Toxicology* 209 (2005) 225–235.
- [36] P. Ragavendran, A. Sophia, A. Arulraj, V.K. Gopalakrishnan, Cardioprotective effect of aqueous, ethanol and aqueous ethanol extract of *Aerva lanata* (Linn.) against doxorubicin induced cardiomyopathy in rats, *Asian Pac. J. Trop. Biomed.* 2 (2012) 12–18.
- [37] S. Ramachandran, N. Rajendra Prasad, S. Karthikeyan, Sesamol inhibits UVB-induced ROS generation and subsequent oxidative damage in cultured human skin dermal fibroblasts, *Arch. Dermatol. Res.* 302 (2010) 733–744.
- [38] J.L. Ryan, Ionizing radiation: the good, the Bad, and the ugly, *J. Invest. Dermatol.* 132 (2012) 985–993.
- [39] A.K. Sachdeva, S. Misra, I. Pal Kaur, K. Chopra, Neuroprotective potential of sesamol and its loaded solid lipid nanoparticles in ICV-STZ-induced cognitive deficits: behavioral and biochemical evidence, *Eur. J. Pharmacol.* 747 (2015) 132–140.
- [40] S. Sharma, I.P. Kaur, Development and evaluation of sesamol as an antiaging agent, *Int. J. Dermatol.* 45 (2006) 200–208.

- [41] N. Singh, N. Khullar, V. Kakkar, I.P. Kaur, Hepatoprotective effects of sesamol loaded solid lipid nanoparticles in carbon tetrachloride induced sub-chronic hepatotoxicity in rats, *Environ. Toxicol.* (2014).
- [42] D.M. Small, J.S. Coombes, N. Bennett, D.W. Johnson, G.C. Gobe, Oxidative stress, anti-oxidant therapies and chronic kidney disease, *Nephrology* 17 (2012) 311–321.
- [43] V. Sosa, T. Moline, R. Somoza, R. Paciucci, H. Kondoh, M.E. LLeonart, Oxidative stress and cancer: an overview, *Ageing Res. Rev.* 12 (2013) 376–390.
- [44] Y. Tarumoto, M. Kimura, H. Tokado, R. Shinozawa, T. Tsuchida, K. Noda, S. Nakane, M. Sasajima, M. Ohzeki, Studies of toxicity of hydrocortisone 17-butyrate 21-propionate-5. Chronic toxicity in rats by percutaneous administration (author's transl), *J. Toxicol. Sci.* 6 (Suppl) (1981) 97–120.
- [45] B. Uttara, A.V. Singh, P. Zamboni, R.T. Mahajan, Oxidative stress and neurodegenerative diseases: a review of upstream and downstream antioxidant therapeutic options, *Current Neuropharmacol.* 7 (2009) 65–74.